Compound Second-order hyperbolic partial differential equation-based structural interpolation model

T. Barbu

Abstract. A novel partial differential equation (PDE) - based structural image interpolation technique is proposed in this work. It is based on a nonlinear hyperbolic PDE model that successfully inpaints the image by directing the diffusion mostly to the missing regions, using a second-order anisotropic diffusion component and an inpainting mask. It also contains a component that combines the evolving image to a 2D filter kernel. The proposed hybrid PDE model is well-posed and numerically solved using an explicit iterative finite difference-based numerical approximation scheme that is stable, consistent to the hyperbolic model and converges to its weak solution. Some experiments and method comparison illustrating the effectiveness of the inpainting method are also described.

M.S.C. 2010: 35Lxx, 35L70, 60G35, 65L12, 68U10, 94A08
Key words: structural inpainting; nonlinear hyperbolic PDE model; second-order anisotropic diffusion; 2D filter kernel; finite difference method; numerical approximation algorithm.

1 Introduction

Digital inpainting, also known as image interpolation or completion, represents the computer-based process that reconstructs automatically the missing parts of the image using the known information around them. Inpainting represents an ancient term having its origin in the art restoration [1]. The main application areas of image interpolation are the following: deteriorated painting reconstruction, photo and movie restoration, image and video object removal or replacing, zooming and super-resolution, solving the disocclusion task, estimating the scene behind an obscuring foreground, and the image compression and decompression tasks [1].

We distinguish here three categories of interpolation techniques: texture-based, structure-based and combined inpainting algorithms. Some textural reconstruction methods are based on the texture synthesis [2], while many other represent exemplar-based interpolation algorithms [3].

Applied Sciences, Vol. 21, 2019, pp. 27-33.

Structural inpainting employs information around the missing region to estimate the isophotes (level lines) from coarse to fine, and diffuses information by the diffusion mechanism. It is performed by using the partial differential equation (PDE)-based and the energy-based (variational) models [4].

The state of the art variational inpainting techniques include those based on Mumford-Shah model [5], the Harmonic Inpainting model [6], Total Variation Inpainting [7] and its improved versions [8], [9], [10], [11], and Euler Elastica Inpainting Model [12]. Also, many nonlinear PDE-based inpainting models of various orders have been developed in the last decades. Some of them follow the variational principle, while other PDE interpolation models are not derived from variational schemes, being directly given as evolutionary equations. Let us mention here the third-order PDE-based models, such as Curvature-driven Diffusion (CDD) Inpainting [13], and the fourth-order PDE inpainting schemes, like Cahn-Hillard Inpainting [14], TVH-1 Inpainting [15] and LCIS Inpainting [16].

We also proposed numerous variational and PDE-based inpainting techniques in our past papers [17], [18], [19]. Here we consider a nonlinear second-order hyperbolic PDE-based inpainting technique combining an anisotropic diffusion term to a two-dimension conventional filter kernel. The proposed hybrid interpolation solution provides effective reconstruction results, enhance the image details and works successfully in noisy conditions also.

The considered differential model is described in the next section. Then, it is solved numerically, by applying the finite-difference method, in the third section. Some experiments and method comparison ar discussed in the fourth section, while the conclusions of this work are drawn in the fifth section.

2 A combined hyperbolic PDE-based inpainting model

A novel second-order nonlinear hyperbolic PDE-based image interpolation framework is considered here. The image that is evolving in the structural inpainting process is represented as the next partial 2D function: $u : \Omega \to R$, $u|_{\Omega\setminus\Gamma} = u_0$, where $\Omega \subseteq R^2$ is the image domain and the inpainting region $\Gamma \subset \Omega$.

Thus, we construct the next second-order hyperbolic partial differential equation with several boundary conditions:

$$\begin{cases} \alpha \dfrac{\partial^2 u}{\partial t^2} + \beta^2 \dfrac{\partial u}{\partial t} - \gamma(\|\nabla u * G_\sigma\|)\nabla \cdot (\psi(|\nabla u|)\nabla u) + \lambda(1 - 1_\Gamma)(u - u_0) = 0 \\ u(0, x, y) = u_0(x, y) \\ \dfrac{\partial u}{\partial t}(0, x, y) = u_1(x, y) \\ u(t, x, y) = 0, \ \forall (x, y) \in \partial\Omega \setminus \Gamma \end{cases} \tag{2.1}$$

where $\alpha, \beta, \lambda \in (0, 1]$.

The anisotropic diffusion component of this model, $\nabla \cdot (\psi(|\nabla u|)\nabla u)$, is based on the following diffusivity function:

$$\psi : [0, \infty) \to [0, \infty), \psi(s) = \delta \left(\frac{\xi(u)}{\eta \ln(s + \xi(u))^k + \varepsilon} \right)^{1/3}, \tag{2.2}$$

where the conductance parameter is

$$\xi(u) = \|r\mu(|\nabla u\|) - t\nu\| \tag{2.3}$$

with $\delta, \eta, \nu \in (0,1),\ k \in \{1,2,3,4\},\ \varepsilon, r \in (1,5]$ and μ returns the average of the argument. This diffusivity function has the properties required by an effective restoration process: positive, monotonically decreasing and convergent to 0 [4].

Another component is controlling the speed of the diffusion process and enhances the boundaries. It is based on the following function:

$$\gamma : [0,\infty) \to [0,\infty),\ \gamma(s) = \zeta\ \sqrt[m+1]{\rho s^m + \xi} \tag{2.4}$$

where $\zeta, \rho, \xi \in (0,6)$ and $m \in (0,3)$. The term combines by convolution the evolving image u to a 2D conventional filter kernel. We may choose the next two-dimension Gaussian filter [20]:

$$G_\sigma(x,y) = \frac{1}{2\pi\sigma}\ e^{-\frac{x^2+y^2}{2\sigma^2}} \tag{2.5}$$

The PDE model (2.1) inpaints the image successfully by directing the diffusion mostly to the missing, or highly damaged, parts (inpainting region), using the inpainting mask given by the characteristic function of Γ. Also, since it is based on the second-time derivative, given its hyperbolic character, this PDE removes successfully the diffusion effect in the vicinity of the edges, thus producing sharper boundaries and better details.

This combined nonlinear hyperbolic diffusion-based model is well-posed, admitting a unique weak solution, representing the reconstructed image. That solution is computed by applying a numerical approximation scheme that is proposed in the following section.

3 An iterative numerical approximation algorithm

The proposed nonlinear hyperbolic PDE model is solved numerically by applying the finite difference method [21]. So, we propose an effective finite difference-based numerical approximation scheme for it.

We construct a grid, quantizing the time and space coordinates as following: $x = ih,\ y = jh,\ t = n\Delta t,\ i \in \{1,...,I\},\ j \in \{1,...,J\},\ n \in \{0,...,N\}$. The hyperbolic PDE in (2.1) leads to:

$$\begin{aligned} &\alpha\ \frac{\partial^2 u}{\partial t^2} + \beta^2\ \frac{\partial u}{\partial t} - \lambda(1-1_\Gamma)(u-u_0) \\ &\qquad = \gamma(\|\nabla u * G_\sigma\|)\left(\frac{\partial}{\partial x}(\psi(|\nabla u|)u_x) + \frac{\partial}{\partial y}\ (\psi(|\nabla u|)u_y)\right) \end{aligned} \tag{3.1}$$

The left term of (3.1) is discretized using finite differences [21], as follows:

$$\begin{aligned} &\alpha\ \frac{u_{i,j}^{n+\Delta t} + 2u_{i,j}^n - u_{i,j}^{n-\Delta t}}{(\Delta t)^2} + \beta^2\ \frac{u_{i,j}^{n+\Delta t} - u_{i,j}^n}{\Delta t} + \lambda(1-1_\Gamma)(u_{i,j}^n - u_{i,j}^0) \\ &\quad = u_{i,j}^{n+\Delta t}\ \frac{(\alpha + \beta^2\Delta t)}{(\Delta t)^2} + u_{i,j}^n\ \frac{2\alpha - \beta^2\Delta t + \lambda(1-1_\Gamma)(\Delta t)^2}{(\Delta t)^2} \\ &\quad -u_{i,j}^{n-\Delta t}\ \frac{\alpha}{(\Delta t)^2} - u_{i,j}^0\lambda(1-1_\Gamma) \end{aligned} \tag{3.2}$$

Then, the right term is approximated numerically, by using central differences [21]. Thus, one first computes $\gamma_{i,j}=\gamma(\|u*G_\sigma)_{i,j}\|)$ and $\psi_{i,j}=\psi(\|u_{i,j}\|)$, where $\|u_{i,j}\|\approx\sqrt{\left(\frac{u_{i+h,j}-u_{i-h,j}}{2h}\right)^2+\left(\frac{u_{i,j+h}-u_{i,j-h}}{2h}\right)^2}$. Next, $\frac{\partial}{\partial x}\ (\psi(\|\nabla u\|)u_x)$ is discretized spatially as $\psi_{i+\frac{h}{2},j}(u_{i+h,j}-u_{i,j})-\psi_{i-\frac{h}{2},j}(u_{i,j}-u_{i-h,j})$, while $\frac{\partial}{\partial y}\ (\psi(\|\nabla u\|)u_y)$ is discretized spatially as $\psi_{i,j+\frac{h}{2}}(u_{i,j+h}-u_{i,j})-\psi_{i,j-\frac{h}{2}}(u_{i,j}-u_{i,j-h})$, where $\psi_{i\pm\frac{h}{2},j}=\frac{\psi_{i\pm h,j}+\psi_{i,j}}{2}$, $\psi_{i,j\pm\frac{h}{2}}=\frac{\psi_{i,j\pm h}+\psi_{i,j}}{2}$.

We may consider the values $h=\Delta t=1$ and obtain the following implicit approximation:

$$\begin{aligned}&u_{i,j}^{n+1}(\alpha+\beta^2)+u_{i,j}^n(2\alpha-\beta^2+\lambda(1-1_\Gamma))-u_{i,j}^{n-1}\alpha-u_{i,j}^0\lambda(1-1_\Gamma)\\&=\gamma_{i,j}(\psi_{i+\frac{1}{2},j}(u_{i+1,j}^n-u_{i,j}^n)-\psi_{i-\frac{h}{2},j}(u_{i,j}^n-u_{i-1,j}^n)\\&+\psi_{i,j+\frac{1}{2}}(u_{i,j+1}^n-u_{i,j}^n)-\psi_{i,j-\frac{1}{2}}(u_{i,j}^n-u_{i,j-1}^n))\end{aligned}\tag{3.3}$$

It then leads to the next explicit iterative numerical approximation scheme:

$$u_{i,j}^{n+1}=\frac{1}{\alpha+\beta^2}\left(\begin{array}{l}u_{i,j}^n(\beta^2-2\alpha-\lambda(1-1_\Gamma)-\gamma_{i,j}(\psi_{i+\frac{1}{2},j}+\psi_{i-\frac{1}{2},j}+\psi_{i,j+\frac{1}{2}}+\psi_{i,j-\frac{1}{2}}))\\+u_{i+1,j}^n\psi_{i+\frac{1}{2},j}\gamma_{i,j}+u_{i-1,j}^n\psi_{i-\frac{h}{2},j}\gamma_{i,j}+u_{i,j+1}^n\psi_{i,j+\frac{1}{2}}\gamma_{i,j}\\+u_{i,j-1}^n\psi_{i,j-\frac{1}{2}}\gamma_{i,j}\\+u_{i,j}^{n-1}\alpha+u_{i,j}^0\lambda(1-1_\Gamma)\end{array}\right)\tag{3.4}$$

This explicit numerical approximation algorithm is stable and consistent to the nonlinear hyperbolic PDE model (2.1). It is converging quite fast, in N iterations, to its weak solution representing the inpainted image.

4 Interpolation experiments and method comparison

The combined nonlinear hyperbolic PDE-based inpainting technique described here has been tested on hundreds of images affected by missing zones, successfully reconstruction results being achieved. The three volumes of the USC-SIPI database and other important image collections have been used in our interpolation experiments.

The iterative numerical discretization algorithm (3.4) that is used in the experiments converges quite fast, the number of steps, N, being rather low. However, the execution time is influenced by the size of the inpainting region. It provides a proper reconstruction of the damaged image, filling successfully the missing regions, and works well in noisy conditions too, given the combination to the 2D Gaussian filter kernel. It reduces the additive noise and the undesired effects, preserving the edges and image features very well. As already mentioned, given its hyperbolic character, this interpolation method provides sharper boundaries.

Structural inpainting method comparisons have been also performed by us. The performance of our interpolation framework has been assessed using the Peak Signal-to-Noise Ratio (PSNR) metric [22].

The proposed approach outperforms many existing inpainting models, providing better results for non-textured images affected by missing parts in both clean

and noisy conditions. However, it does not reconstruct properly the textures, being outperformed by other methods in this case. Averaged PSNR values achieved by some structure-based inpainting approaches are displayed in Table 1. Our algorithm achieves higher PSNR values than some state-of-the-art methods.

Table 1. PSNR values of several methods

Inpainting technique	Average PSNR
This hyperbolic PDE model	31.07 (dB)
Harmonic Inpainting	27.31 (dB)
TV Inpainting	28.56 (dB)
CDD Inpainting	30.65 (dB)

An image inpainting example is described in Figure 1. The original *Mandrill* image is displayed in (a). The image affected by a missing region, representing several black scratches, and an amount of white additive Gausian noise is depicted in (b).

The image inpainted by the described approach is depicted in (c), the TV Inpainting output is displayed in (d), the completion using Harmonic Inpainting in (e) and the CDD Inpainting in (f).

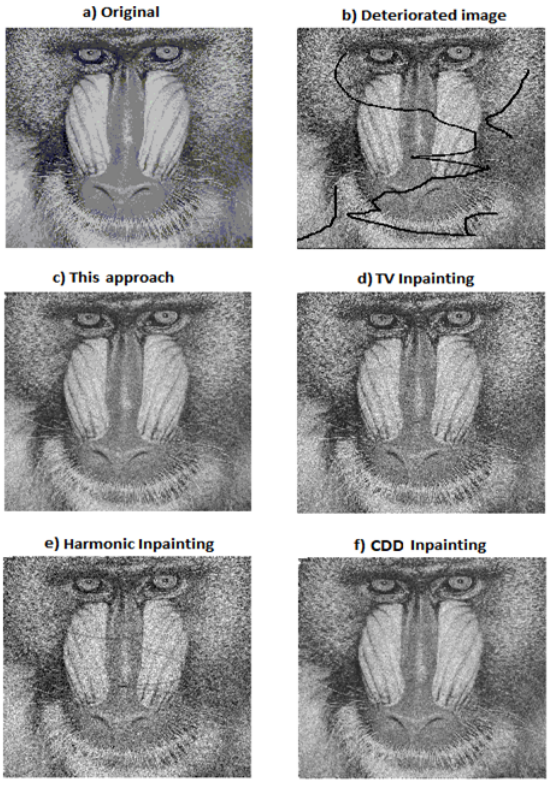

Figure 1: *Mandrill* image inpainted by several methods

5 Conclusions

A nonlinear hyperbolic second-order PDE-based structural inpainting technique has been described in this work. It is based on a combined PDE model composed of a nonlinear diffusion term using a novel edge-stopping function, which assures a detail-preserving restoration directed to the inpainting region given by the mask, and a component combining the evolving image to a filtering kernel, which controls the speed of the diffusion process.

The explicit iterative numerical approximation scheme constructed for this differential model by applying the finite-difference method represents another contribution of this paper. The developed completion approach sucessfully inpaints the image in both normal and noisy conditions. So, it reduces the additive noise and alleviate some undesired effects like blurring and staircasing.

It also provides a better structure-based interpolation than many state of the art diffusion-based techniques. Unfortunately, the proposed algorithm achieves much weaker results for texture-based inpainting. Thus, we are going to further improve this model as part of our future research, by extending this technique in the direction of the textural image interpolation.

References

[1] C.B. Schonlieb, *Partial Differential Equation Methods for Image Inpainting*, Volume 29, Cambridge University Press, 2015.

[2] A.A. Efros, T.K. Leung, *Texture synthesis by non-parametric sampling*, Proceedings of the International Conference on Computer Vision 2 (1999), 1033.

[3] A. Criminisi, P. Perez, K. Toyama, *Region filling and object removal by exemplar-based image inpainting*, IEEE Transactions on Image Processing 13 (9) (2004), 1200-1212.

[4] B. Song, *Topics in Variational PDE Image Segmentation, Inpainting and Denoising*, University of California, 2003.

[5] S. Esedoglu, J. Shen, *Digital inpainting based on the Mumford-Shah Euler image model*, European Journal of Applied Mathematics, 2002.

[6] K.T. Inoue, P. Cabella, E. Komatsu, *Harmonic inpainting of the cosmic microwave background sky: Formulation and error estimate*, Physical Review D 77 (June, 2008).

[7] T.F. Chan, J. Shen, *Morphologically invariant PDE inpaintings*, UCLA CAM Report, 2001, 1–15.

[8] P. Getreuer, *Total variation inpainting using split Bregman*, Image Processing On Line, 2 (2012), 147-157.

[9] M.V. Afonso, J.M.R. Sanches, *Blind inpainting using l0 and total variation regularization*, IEEE Transactions on Image Processing 24 (7) (2015), 2239-2253.

[10] M. Neri, E.R. Zara, *Total variation-based image inpainting and denoising using a primal-dual active set method*, Philippine Science Letters 7 (1) (2014), 97-103.

[11] K. Bredies, M. Holler, *A TGV-based framework for variational image decompression, zooming, and reconstruction*, Part I: *Analytics*, SIAM J. Imag. Sci. 8 (4) (2015), 28142850.

[12] T.F. Chan, S.-H. Kang, J. Shen, *Eulers elastica and curvature based inpaintings*, SIAM J. Appl. Math. 2002.

[13] T.F. Chan, J. Shen, *Non-texture inpainting by curvature-driven diffusions* (CDD), J. Visual Comm. Image Rep. 4 (12) (2001), 436-449.

[14] M. Burger, L. He, C. Schonlieb, *Cahn-Hilliard inpainting and a generalization for grayvalue images*, SIAM J. Imaging Sci. 2 (4) (2009), 1129-1167.

[15] S. Osher, A. Sole, L. Vese, *Image decomposition and restoration using total variation minimization and the H-1 norm*, Multiscale Modeling and Simulation: A SIAM Interdisciplinary Journal 1 (3) (2003), 349-370.

[16] C.B. Schoenlieb, A. Bertozzi, *Unconditionally stable schemes for higher order inpainting*, Comm. Math. Sci. 2 (9) (2011), 413-457.

[17] T. Barbu, *Variational image inpainting technique based on nonlinear second-order diffusions*, Computers & Electrical Engineering 54 (2016), 345-353.

[18] T. Barbu, *Second-order anisotropic diffusion-based framework for structural inpainting*, Proceedings of the Romanian Academy, Series A: Mathematics, Physics, Technical Sciences, Information Science, 19 (2) (2018), 329-336.

[19] T. Barbu, *Novel Diffusion-Based Models for Image Restoration and Interpolation*, Series: Signals and Communication Technology, Springer International Publishing, August 2018.

[20] R. Gonzalez, R. Woods, *Digital Image Processing*, Prentice Hall, 2nd ed., 2001.

[21] D. Gleich, *Finite Calculus: A Tutorial for Solving Nasty Sums*, Stanford University, 2005.

[22] K. H. Thung, P. Raveendran, *A survey of image quality measures*, Proc. of the International Conference for Technical Postgraduates (TECHPOS), 2009, 1-4.

Author's address:

Tudor Barbu
Institute of Computer Science of the Romanian Academy,
Iasi, Romania.
E-mail: tudor.barbu@iit.academiaromana-is.ro